Vol. 609: 87–99, 2019
https://doi.org/10.3354/meps12836

MARINE ECOLOGY PROGRESS SERIES
Mar Ecol Prog Ser

Published January 17

Biological regulation of pH during intensive growth of phytoplankton in two eutrophic estuarine waters

Yafeng Zhang[1,2], Yonghui Gao[2], David L. Kirchman[3], Matthew T. Cottrell[3], Rong Chen[1], Kuo Wang[1], Zhangxian Ouyang[2], Yuan-Yuan Xu[2], Baoshan Chen[2], Kedong Yin[1,*], Wei-Jun Cai[2,*]

[1]School of Marine Sciences, Sun Yat-Sen University, Guangzhou 510006, PR China
[2]School of Marine Science and Policy, University of Delaware, Newark, Delaware 19716, USA
[3]School of Marine Science and Policy, University of Delaware, Lewes, Delaware 19958, USA

ABSTRACT: Estuarine inorganic eutrophication results in high biomass of phytoplankton and elevates pH in the surface layer. However, its effects on the carbonate system are not well understood. We conducted incubation experiments using low-, moderate- and high-salinity waters enriched with nutrients in Delaware Bay and the Pearl River Estuary to examine effects on the carbonate system. The results showed that as phytoplankton grew, pH increased and dissolved inorganic carbon (DIC) decreased. However, the decrease in DIC was not fully accounted for by the production of organic carbon. This indicates that some C was missing during high phytoplankton growth. The missing C appeared to depend on the water buffering capacity, as it was largest when pH was highest in the low-salinity estuarine water. Total alkalinity (TA) decreased more in the low-salinity water with nutrient additions in both estuaries. We proposed that carbonate precipitation was formed at high pH driven by high phytoplankton growth, which is confirmed by a model simulation of TA. The model simulation based on the stoichiometric ratio of −Δ106DIC: Δ17TA demonstrated the difference between simulated and observed TA. The difference disappeared when carbonate precipitation formation was considered in the model, indicating carbonate precipitation formation could account for the missing C, the decrease in TA and the increase in pH. We concluded that the mechanism of CO_2 being released from carbonate precipitation due to bloom-induced high pH benefits further photosynthesis, thus enhancing the biological pump efficiency in estuarine and coastal ecosystems.

KEY WORDS: Phytoplankton blooms · pH · Dissolved inorganic carbon · Total alkalinity · Estuary

1. INTRODUCTION

Ocean acidification has raised questions of how the declining oceanic pH induced by fossil CO_2 may interact with the larger natural variations of pH in eutrophic coastal and estuarine marine ecosystems (Feely et al. 2010, Cai et al. 2011, Duarte et al. 2013). Because of the increased input of anthropogenic nutrients from runoff, phytoplankton blooms have increased in frequency and magnitude, playing a more important role in carbon input and transformation in estuarine and coastal ecosystems (Howarth 1988, Cloern et al. 2014, Carstensen et al. 2015), particularly in eutrophic estuaries (Chen et al. 2003, Yin 2003). Eutrophication, amplifying both production and respiration of organic carbon, has the potential to reduce or exacerbate the impacts of ocean acidification in coastal waters (Doney et al. 2007, Borges &

*Corresponding authors: yinkd@mail.sysu.edu.cn, wcai@udel.edu

Gypens 2010, Cai et al. 2017), resulting in more complex dynamics of pH (Hinga 2002, Duarte et al. 2013, Flynn et al. 2015). Indeed, dense phytoplankton blooms can deplete dissolved CO_2 and raise pH to as high as 10 in the surface layer of coastal and estuarine waters (Hansen 2002, Björk et al. 2004, Gao et al. 2014). It is common that laboratory cultures of phytoplankton raise pH above 10 and cause carbon limitation (Middelboe & Hansen 2007, Verschoor et al. 2013).

High biomass growth of phytoplankton has complex effects on dissolved inorganic carbon (DIC), pH, total alkalinity (TA) and carbonate precipitation (Vandamme et al. 2012, Verspagen et al. 2014). Although DIC uptake by phytoplankton does not affect TA, proton consumption during NO_3^- and PO_4^{3-} uptake increases TA (Wolf-Gladrow et al. 2007). Importantly, an increase in pH and TA may shift DIC composition from HCO_3^- to CO_3^{2-} dominance, which favors mineral precipitation such as calcium carbonate. The process of mineral precipitation not only reduces TA and pH but also releases CO_2 (Frankignoulle et al. 1994, Soetaert et al. 2007, Vandamme et al. 2012), which could then benefit further biological production. Although many interactions between phytoplankton and DIC chemistry have been examined, the coupled feedbacks between phytoplankton growth and carbonate chemistry as reflected in changes in DIC, pH and TA are not straightforward and have received little attention.

The Pearl River, the second largest river discharge in China, is characterized by heavy eutrophication due to inorganic nutrient enrichment from municipal and livestock waste discharges. The river freshwater flows out in the northern South China Sea. Upstream, phytoplankton growth is mainly limited by light, as the freshwater in the riverine plume is turbid, whereas the South China Sea water is oligotrophic and, hence, phytoplankton growth is limited primarily by nutrients (Yin et al. 2004, Yin & Harrison 2008). The estuarine plume is a mixture of riverine water and seawater and has high nutrients and improved light penetration. Therefore, phytoplankton blooms often occur in the estuarine plume, and the magnitude of the blooming biomass is restricted by phosphorus as the most limiting nutrient (Yin 2003, Lu & Gan 2015). There has been no seasonal large-scale hypoxia in Pearl River estuarine coastal waters.

Delaware Bay is an urbanized estuary in the eastern USA and in the past had suffered from summer hypoxia mainly due to municipal and industrial inputs in the urban region (Kauffman et al. 2011). Although water quality has been remarkably improved over the past 2 decades, nutrient loading is still high and phytoplankton blooms still occur in the middle to lower estuary (Sharp et al. 2009). A field investigation observed that a net DIC drawdown of 100 to 150 µmol kg^{-1} and a TA increase of 0 to 50 µmol kg^{-1} were estimated during a phytoplankton bloom with 0.2 to 1.8 µg l^{-1} chl *a* in the Pearl River Estuary (Dai et al. 2008). In Delaware Bay, a slight DIC removal has also been observed in the mid-bay, where chl *a* content is high (Sharp et al. 2009, Joesoef et al. 2015, 2017).

High pH in seawater can result in mineral precipitation, which can change the balance between TA, DIC and pH since the 3 variables are intimately linked. Phytoplankton uptake of CO_2 is a driver for the feedback process. For example, high levels of particulate inorganic carbon were reported in the Loire Estuary, where chl *a* reached as high as 80 µg l^{-1} (Abril et al. 2003). Therefore, the coupled feedbacks between phytoplankton growth and carbonate chemistry are related to the magnitude of phytoplankton biomass. However, the process of feedback regulation by phytoplankton growth is not well understood. To eliminate variation in freshwater flow, water column stability, light limitation and other environmental factors on growth of phytoplankton, we conducted bottle incubation experiments in both Delaware Bay and the Pearl River Estuary to examine the phytoplankton growth regulated process of the coupling relationships between phytoplankton growth, TA, DIC and pH during high biomass phytoplankton growth in the 3 different water salinities, which represent the different buffering capacities of the waters.

2. MATERIALS AND METHODS

2.1. Incubation experiment design and water sampling sites

Incubation experiments were set up using waters from Delaware Bay and the Pearl River Estuary. There were 3 sets of incubation experiments containing low-salinity, moderate-salinity and high-salinity waters, among which intermediate-salinity water was a mixture of the other 2 waters. Some treatments received additions of nutrients (NO_3-N, SiO_3-Si and PO_4-P), and all treatments were incubated for 5 d, during which time samples were taken for various parameters.

In Delaware Bay, we took surface water samples (0.5 m depth) at a river site (39° 42′ 43″ N, 75° 30′ 51″ W;

salinity = 0.21 in May and 0.62 in August 2015) and another estuarine site (38° 47′ 13″ N, 75° 06′ 06″ W; salinity = 28.91 in May and 29.29 in August 2015). All water samples were filtered through 200 µm mesh to remove mesozooplankton. Moderate-salinity water was prepared by mixing equal portions of low- and high-salinity waters (final salinity = 15.22 in May and 15.53 in August 2015). For the August incubation experiments, nutrients were added to the samples (final concentration of 100 µM NO_3-N, 6 µM PO_4-P, 100 µM SiO_3-Si), but nutrients were not added for the May incubation experiments. All sample waters were transferred into 300 ml BOD bottles. All incubation bottles, tubes and carboys were washed with 10% HCl and rinsed thoroughly with distilled water and sample water before the experiments. The bottles were covered with neutral density screen to reduce the light intensity to 50% of the surface value (about 1200 µmol m^{-2} s^{-1} at noon) and incubated outdoors at 25 ± 1°C maintained with a circulating water bath. Each day at 07:00, 13:00 and 19:00 h, 3 bottles for each treatment were sacrificed for samples of pH, DIC, TA, nutrients and chl *a*.

In the Pearl River Estuary, we took surface water samples (0.5 m depth) at a river site (22° 49′ 16″ N, 113° 34′ 00″ E; salinity = 2.86) and another estuarine site (22° 0′ 34″ N, 113° 53′ 13″ E; salinity = 31.71) in December 2015. The samples were collected, prepared and enriched with nutrients in the same way as those in the Delaware Bay experiments. The salinity of the mixture of freshwater and seawater was 17.23. Sample waters were placed into 2.5 l polycarbonate bottles and incubated in a culture room with 24 h light at 500 µmol m^{-2} s^{-1} and at 25°C. The temperature condition was comparable to and the light was weaker than that in Delaware Bay. Each day at 13:00 h, 2 polycarbonate bottles for each treatment were sacrificed to measure pH, DIC, TA, nutrients and chl *a*. Also, we collected samples for particulate organic carbon (POC) and dissolved organic carbon (DOC).

2.2. Sample analysis

Samples for DIC and TA were preserved with $HgCl_2$ in 60 ml borosilicate glass bottles (final concentration: 0.04% saturated $HgCl_2$) for later analysis. DIC and TA were analyzed using established methods (Cai et al. 2003, Huang et al. 2012), and the precision for DIC and TA was 0.1 and 0.3%, respectively. pH was measured in gas-tight vials with a Ross combination glass electrode at 25°C against the NIST scale within 2 h of sampling. For chl *a*, 80 to 100 ml water samples were filtered through GF/F filters, and the filters were stored in the dark at −20°C. Chl *a* concentrations were estimated by fluorometry after acetone extraction overnight at 4°C (Knap et al. 1996). For nutrients, filtered water was stored at −20°C until measurements were carried out with a nutrient analyzer (Delaware Bay samples with Skalar San++ autoanalyzer; Pearl River Estuary samples with Futura, Alliance Instruments). For POC, 200 ml of sample water was filtered with combusted GF/F filters (500°C for 5 h). The filters were placed overnight in a desiccator saturated with HCl fumes to remove all calcite and then dried for 5 h at 60°C. POC was analyzed using an elemental analyzer (Knap et al. 1996). DOC in the filtered water was placed in combusted 40 ml borosilicate glass bottles (500°C for 5 h) and stored at −20°C until measurements were carried out with a total organic carbon (TOC) analyzer (Shimadzu TOC-L series) (Knap et al. 1996). Samples for POC and DOC in the Delaware Bay experiments were not collected.

2.3. Model to explore changes in TA and DIC

As given in the simplified TA definition (Eq. 1), photosynthetic uptake of CO_2 does not affect TA, but NO_3^- and PO_4^{3-} assimilation leads to a consumption of H^+ and thus causes a slight increase in alkalinity (Eq. 2). According to the Redfield ratio, 106 mol of DIC uptake consumes 17 H^+ and produces TA by 17 mol, of which 16 mol are from NO_3^- reduction to NH_3 and 1 mol is from proton dissociation from H_3PO_4, as shown in Eq. (2) (Wolf-Gladrow et al. 2007, Cai et al. 2011):

$$TA = [HCO_3^-] + 2[CO_3^{2-}] + [OH^-] - [H^+] \quad (1)$$

$$106CO_2 + 122H_2O + 16HNO_3 + H_3PO_4 \rightarrow (CH_2O)_{106}(NH_3)_{16}(H_3PO_4) + 138O_2 \quad (2)$$

The precipitation of $CaCO_3$ can be described by:

$$Ca^{2+} + 2HCO_3^- \leftrightarrow CaCO_3 + CO_2 + H_2O \quad (3)$$

or equally by:

$$Ca^{2+} + CO_3^{2-} \leftrightarrow CaCO_3 \quad (4)$$

with the 3 DIC species linked by the chemical equilibrium:

$$2HCO_3^- \leftrightarrow CO_3^{2-} + CO_2 + H_2O \quad (5)$$

Based on these equations, 1 mol of $CaCO_3$ precipitation reduces DIC by 1 mol and TA by 2 mol, and 1 mol of CO_2 is potentially released. Because of the chemical equilibrium, less than 1 mol of CO_2 can be

released per mol of $CaCO_3$ deposited in oceanic conditions (Frankignoulle et al. 1994, Soetaert et al. 2007). Therefore, the changes in TA (TA) result from both nutrient consumption ($TA_{production}$) and precipitation ($TA_{precipitation}$):

$$\Delta TA = TA_{end} - TA_{initial} = TA_{production} - TA_{precipitation} \quad (6)$$

So:

$$TA_{precipitation} = TA_{production} - \Delta TA \quad (7)$$

To test our hypothesis that the high pH driven by phytoplankton growth results in carbonate precipitation, we set up a model to simulate the relationship between pH, DIC and TA. For the simulation, an Excel version of CO2SYS (Pierrot et al. 2006) with carbonic acid dissociation constants of Millero (2010) was used.

3. RESULTS

3.1. Chl *a* and pH

In all incubation experiments, chl *a* increased during the incubation (Fig. 1a,b). The increase in chl *a* with nutrient enrichments was larger in Delaware Bay waters than in Pearl River Estuary waters, although initial nutrients in the former were lower than those in the latter (Table 1). Higher nutrients in the Pearl River Estuary only extended the duration of high phytoplankton biomass. Along with the increase in chl *a*, pH increased in all waters during the incubation; the nutrient additions resulted in an even higher increase in pH (Fig. 1c,d). The elevation in pH was highest in the low-salinity water (up to 10.31 and 10.88) and smallest in the high-salinity water (up to 9.70 and 8.90) in Delaware Bay and the Pearl River Estuary, respectively. pH kept increasing even when chl *a* stopped increasing or started to decrease.

3.2. DIC and TA

As phytoplankton grew, DIC decreased in all water salinities in both Delaware Bay and the Pearl River Estuary (Fig. 2a,b). In Delaware Bay, DIC consumption was about 200 µmol kg^{-1} in all treatments without nutrient additions but increased up to 900 µmol kg^{-1} in all treatments with nutrient additions. How-

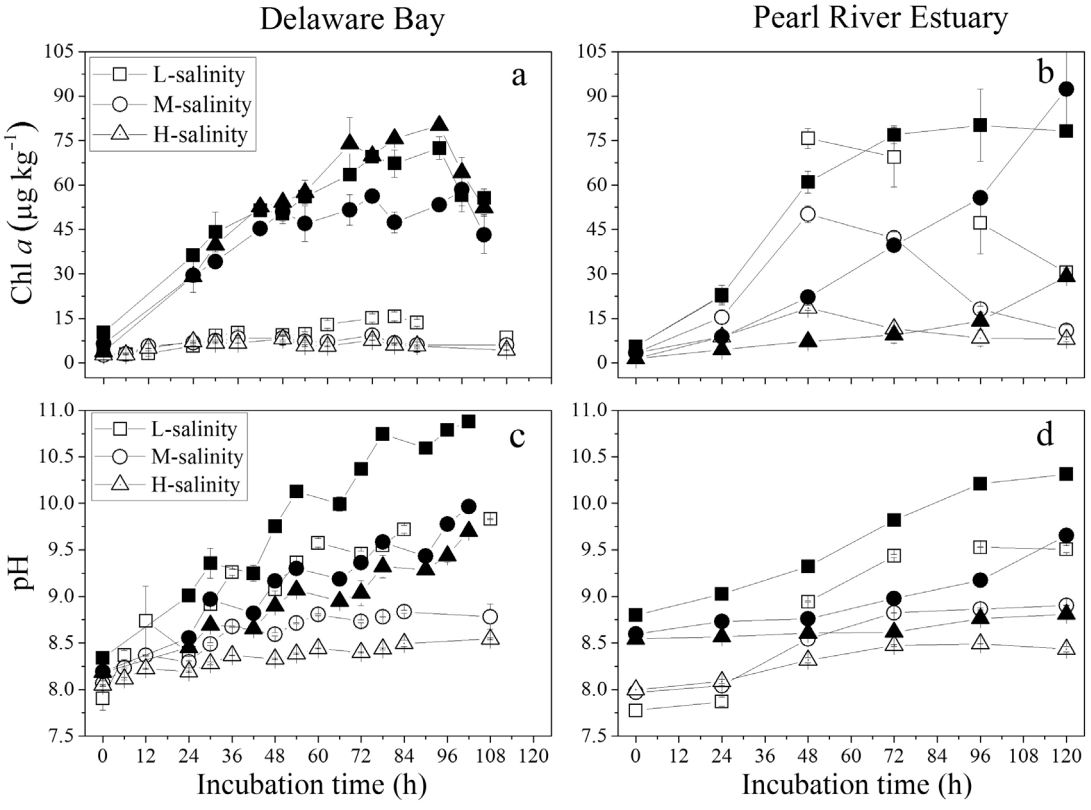

Fig. 1. (a,b) Chl *a* concentrations and (c,d) pH during incubations in 3 water salinities (low, L; moderate, M; high, H) in Delaware Bay and the Pearl River Estuary. Open and solid symbols indicate treatments without and with nutrient additions, respectively; error bars denote SD

Table 1. Initial and end concentrations (mean ± SD) of total inorganic nitrogen (TIN, ammonium + nitrate + nitrite), phosphate (P) and silicate (Si) during incubation in high-salinity (H-Sal), moderate-salinity (M-Sal) and low-salinity (L-Sal) waters in Delaware Bay and the Pearl River Estuary; + indicates nutrient additions

	TIN (μmol kg^{-1})		P (μmol kg^{-1})		Si (μmol kg^{-1})	
	Initial	End	Initial	End	Initial	End
Delaware Bay						
H-Sal	0.64 ± 0.12	0.57 ± 0.01	0.06 ± 0.01	0.02 ± 0.01	3.65 ± 0.70	0.86 ± 0.02
H-Sal+	124.11 ± 7.35	37.08 ± 4.96	6.68 ± 0.42	0.06 ± 0.01	18.71 ± 2.77	5.58 ± 2.29
M-Sal	49.66 ± 5.87	40.97 ± 0.31	0.97 ± 0.11	0.02 ± 0.01	4.26 ± 0.65	9.87 ± 2.51
M-Sal+	150.24 ± 2.88	60.86 ± 3.87	5.61 ± 0.10	0.03 ± 0.01	30.53 ± 0.25	18.40 ± 5.40
L-Sal	105.77 ± 1.56	90.57 ± 0.78	2.06 ± 0.16	0.12 ± 0.01	4.93 ± 0.96	2.30 ± 0.62
L-Sal+	168.72 ± 4.15	31.06 ± 2.31	6.69 ± 0.16	0.13 ± 0.01	44.93 ± 4.27	16.43 ± 5.20
Pearl River Estuary						
H-Sal	26.36 ± 2.52	1.25 ± 0.05	0.38 ± 0.02	0.30 ± 0.02	31.89 ± 3.98	9.20 ± 0.25
H-Sal+	144.89 ± 3.60	86.10 ± 1.23	6.56 ± 0.21	5.08 ± 0.05	207.14 ± 2.45	119.58 ± 4.88
M-Sal	90.66 ± 1.85	48.45 ± 3.65	0.57 ± 0.04	0.31 ± 0.01	90.92 ± 1.33	36.54 ± 1.46
M-Sal+	206.95 ± 3.51	89.55 ± 2.41	6.83 ± 0.24	1.14 ± 0.21	226.88 ± 5.28	33.50 ± 6.88
L-Sal	150.32 ± 2.53	47.05 ± 4.65	0.80 ± 0.11	0.18 ± 0.02	129.51 ± 1.47	55.07 ± 3.81
L-Sal+	200.18 ± 3.12	103.14 ± 0.49	7.01 ± 0.12	0.56 ± 0.02	222.74 ± 2.50	45.55 ± 0.77

ever, in Pearl River Estuary waters, DIC consumption was 590, 470 and 150 μmol kg^{-1} in the low-, moderate- and high-salinity treatments without nutrient additions, respectively, and increased to 860, 770 and 300 μmol kg^{-1} with nutrient additions.

In contrast to DIC and pH, variation in TA was relatively small and complex in the different water salinities (Fig. 2c,d). Generally, in the treatments without nutrient additions, changes in TA (difference between sampling day and initial) were not

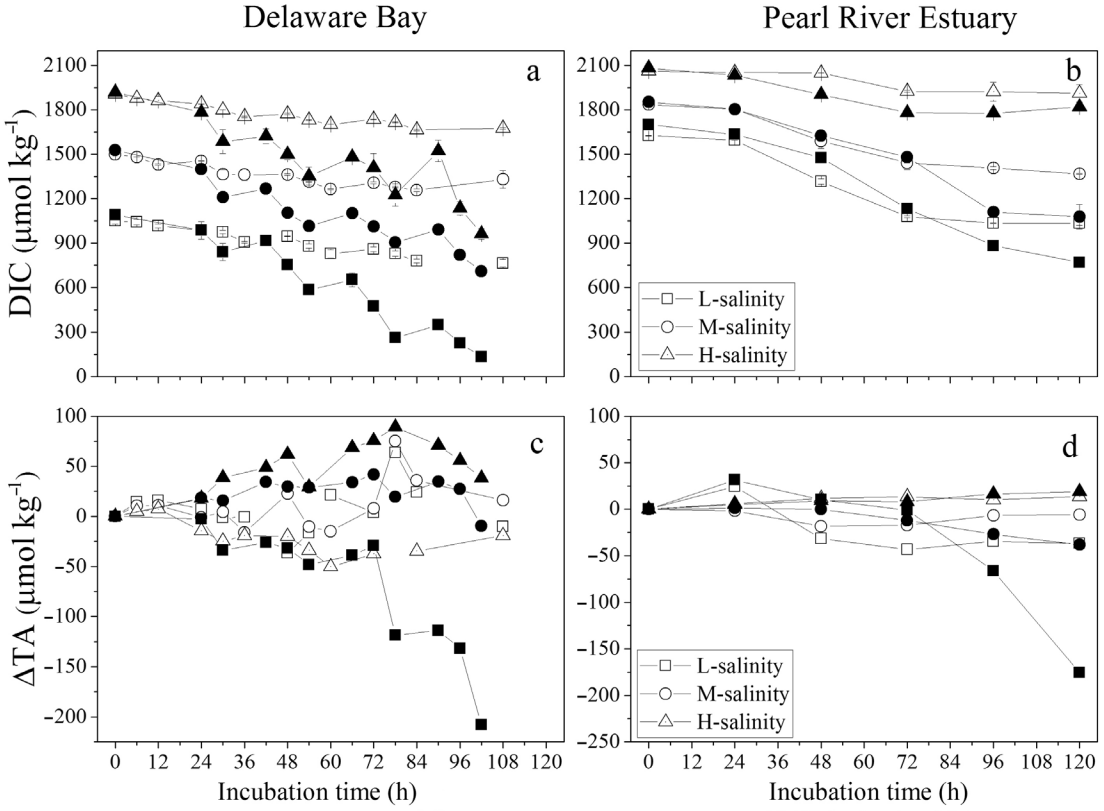

Fig. 2. (a,b) Dissolved inorganic carbon (DIC) and (c,d) total alkalinity (TA) during incubations in 3 water salinities (low, L; moderate, M; high, H) in Delaware Bay and the Pearl River Estuary. ΔTA was TA at the incubated time minus the initial TA for the treatments without (open symbols) and with (solid symbols) nutrient additions; error bars denote SD

Table 2. Decrease in dissolved inorganic carbon:total alkalinity ratios during incubation in high-salinity (H-Sal), moderate-salinity (M-Sal) and low-salinity (L-Sal) waters in Delaware Bay and the Pearl River Estuary. Initial and end ratios are from the beginning and end of incubation, respectively; + indicates nutrient additions

		H-Sal	H-Sal+	M-Sal	M-Sal+	L-Sal	L-Sal+
Delaware Bay	Initial	0.88	0.90	0.92	0.92	0.98	0.98
	End	0.78	0.44	0.75	0.43	0.71	0.23
Pearl River Estuary	Initial	0.90	0.77	0.95	0.82	1.03	0.91
	End	0.79	0.65	0.71	0.49	0.67	0.46

apparent. However, in the treatments with nutrient additions, TA slightly increased at first and then sharply decreased by as much as 200 µmol kg^{-1} in the low-salinity treatments. Changes in TA in the moderate- and high-salinity treatments were less evident in both estuaries. The initial DIC:TA ratios increased as salinity increased, and the ratios decreased in all water salinities during the phytoplankton blooms (Table 2). In addition, the initial DIC:TA ratios in the same water salinities were higher in the Pearl River Estuary than in Delaware Bay. Nutrient additions changed the ratios, particularly in the Pearl River Estuary.

3.3. POC and DOC

As DIC was consumed, both POC and DOC increased (Fig. 3). Organic carbon (POC + DOC) production generally was coupled with chl *a* biomass, but the decrease in DIC was more than the production of organic carbon. This indicates that the decreased DIC was not all transformed into organic carbon and some C was missing. The missing C was highest in the low-salinity treatments (where pH was highest) and lowest in the high-salinity treatments. Nutrient additions increased the amount of missing C in low- and moderate-salinity waters but not in high-salinity water, where phytoplankton chl *a* did not increase much with the addition of nutrients.

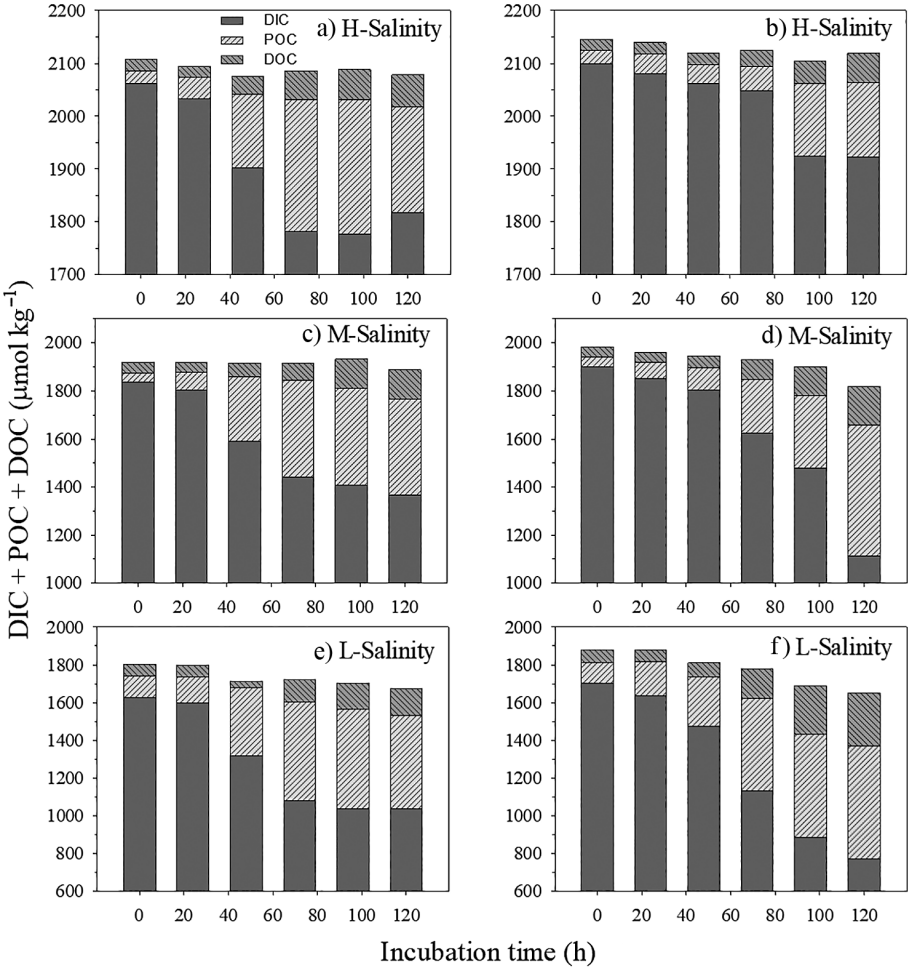

Fig. 3. Dissolved inorganic carbon (DIC), particulate organic carbon (POC) and dissolved organic carbon (DOC) during phytoplankton blooms in 3 water salinities (high, H; moderate, M; low, L) in the Pearl River Estuary. (a,c,e) Treatments without nutrient additions; (b,d,f) treatments with nutrient additions

4. DISCUSSION

4.1. Effect of high phytoplankton biomass bloom on seawater buffering capacity

Seawater pH and carbonate saturation state are determined by the relationship between DIC and TA (Frankignoulle 1994, Egleston et al. 2010, Wang et al. 2013). If DIC equals TA, the system is least buffered, and a slight change in DIC would cause a large change in pH. Generally, DIC and TA are nearly equal in river water, but DIC is less than TA in seawater by 200 to 300 µmol kg^{-1}. Therefore, pH buffering capacity is smaller in freshwater than in seawater. Our study in Delaware Bay and the Pearl River Estuary is consistent with this first-principle-based understanding, though both DIC and TA are higher in the Pearl River Estuary than in Delaware Bay due to the $CaCO_3$ drainage basin in the Pearl River Estuary (Guo et al. 2008, 2009). In addition, DIC:TA ratios decreased in all water salinities because of CO_2 consumption during the intensive growth of phytoplankton in both the Delaware Bay and the Pearl River Estuary experiments (Table 2).

The change in pH or in log(pCO_2) in response to the change in DIC or TA has been used as a measure of how well a system buffers pH or pCO_2 (Frankignoulle 1994, Egleston et al. 2010, Cai et al. 2011). In this study, we used ΔDIC/ΔpH as the overall buffer index to examine how biological removal of DIC and TA affects buffering capacity in different water salinities. A larger buffer index means the buffering capacity is stronger, indicating that the system can accommodate a larger change in DIC for the same unit change in pH. As expected, high-salinity water has a larger buffer index and low-salinity water has a lower buffer index, as buffering capacity increases with decreasing DIC:TA ratios (Fig. 4a). When phytoplankton utilize DIC and amplify the difference between DIC and TA, pH increases and the buffering capacity of the system enhances. In this study, as DIC was consumed by photosynthesis, ΔDIC/ΔpH increased sharply and then stabilized (Fig. 4b), indicating that phytoplankton growth by consuming DIC can enhance the water buffering capacity. In addition, eutrophication by inorganic nutrients would promote consumption of DIC, thus increasing differences between DIC and TA and enhancing the buffering capacity of the system (Table 2, Fig. 4a).

4.2. Effect of carbonate precipitation on high biomass phytoplankton photosynthesis

It is known that photosynthesis elevates pH and shifts DIC towards HCO_3^- and CO_3^{2-} species (Raven 1970, Hansen et al. 2007, Flynn et al. 2012). In this study, CO_2 was already depleted in all water salinities in both Delaware Bay and the Pearl River Estuary when pH increased by about 1 unit (Fig. 5a). Though some phytoplankton species having carbon-concentrating mechanisms can convert HCO_3^- to CO_2 for photosynthesis (Badger et al. 1980, Giordano et al. 2005, Reinfelder 2011), this conversion does not change TA (Eq. 1). Therefore, the decrease in TA in this study suggests another process was involved for

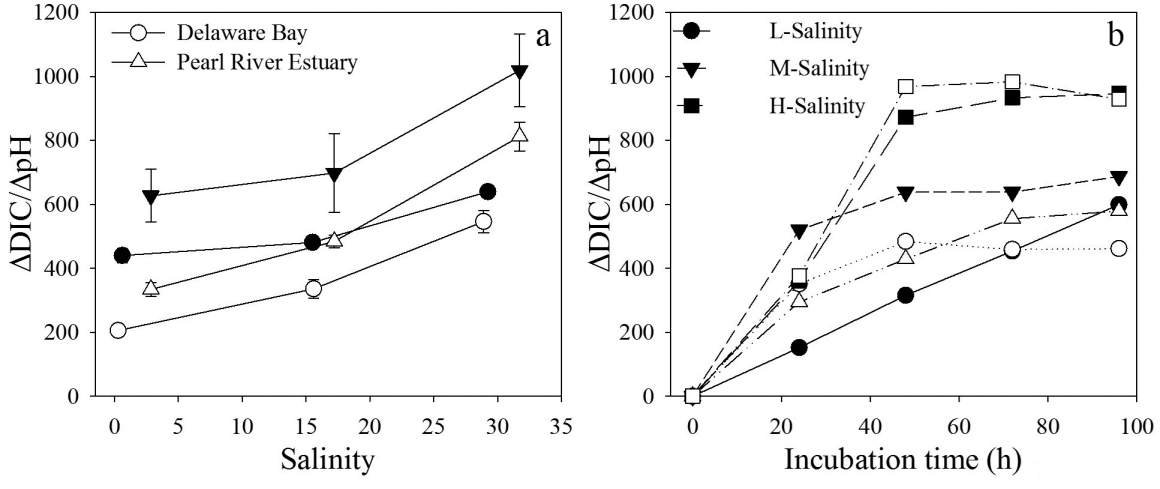

Fig. 4. Estuarine water buffering capacity (ΔDIC/ΔpH) against salinity gradient in Delaware Bay and the Pearl River Estuary. In (a), open and solid symbols indicate treatments without and with nutrient additions, respectively. In (b), open and solid symbols indicate estuarine water buffering capacity (ΔDIC/ΔpH) against incubation time from the Pearl River Estuary and Delaware Bay, respectively. DIC: dissolved inorganic carbon; L: low; M: moderate; H: high

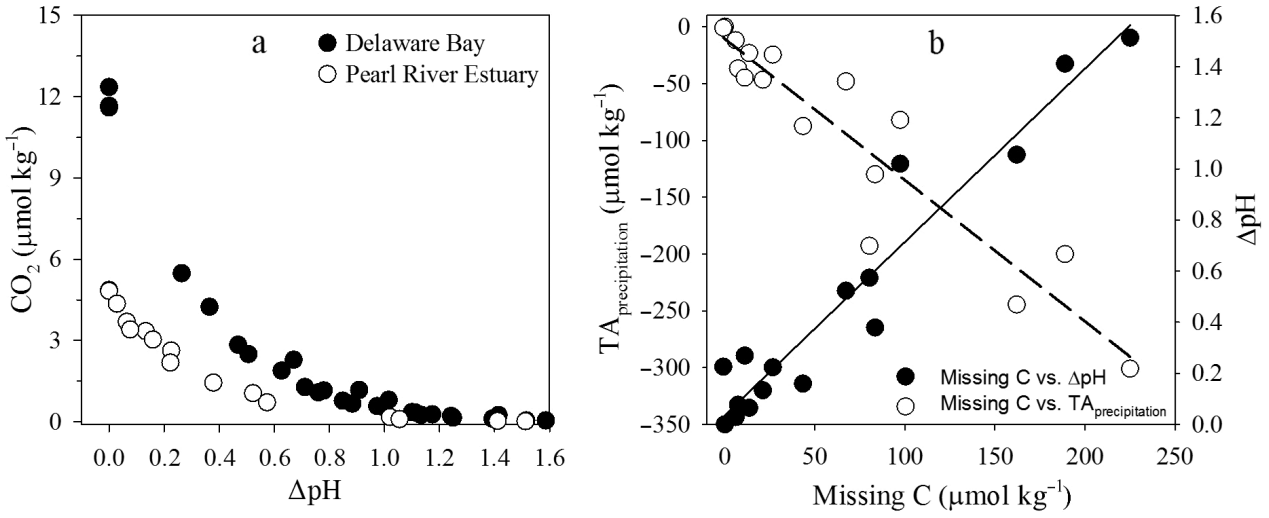

Fig. 5. (a) Simulated concentrations of CO_2 against ΔpH in nutrient addition treatments in Delaware Bay and the Pearl River Estuary. Simulation was carried out with CO2SYS with constants of Millero (2010) (temperature = 25°C). (b) Relationship between missing C and pH ($y = 137.64x - 1.13$, $R^2 = 0.93$, $p < 0.01$) or missing C and precipitated total alkalinity ($TA_{precipitation}$) ($y = -1.24x + 10.55$, $R^2 = 0.88$, $p < 0.01$) in Pearl River Estuary waters with nutrient additions. The missing C is calculated as the difference between the decrease in dissolved inorganic carbon (DIC) and the increase in particulate organic carbon (POC) and dissolved organic carbon (DOC) (missing C = $DIC_{decreased} - POC_{increased} - DOC_{increased}$); $TA_{precipitation} = \Delta TA - TA_{production}$ and $TA_{production}$ were calculated on nitrogen consumption

sustaining the continuous increase in pH in the experiments. The missing C might offer an explanation for this mechanism. Missing C increased with pH, and the ratio of TA reduced by precipitation to missing C is about 1.24, indicating the formation of carbonate precipitation under high pH conditions (Fig. 5b), which is consistent with the sharp increase in aragonite saturation state (Ω_{arag}) values during the phytoplankton bloom in both Delaware Bay and the Pearl River Estuary (Table 3, Fig. 6). Ω_{arag} increased during incubation in the 3 water salinities, with higher Ω_{arag} values at high salinity. At the later stage of the incubation, Ω_{arag} in the low-salinity water decreased when TA decreased because of the occurrence of carbonate precipitation (Fig. 6a). The plot of Ω_{arag} vs. TA production showed that the increase in Ω_{arag} was lower at low salinity than at high salinity (Fig. 6b), indicating that changes in salinity altered the relationships between Ω_{arag} and TA production and influenced the occurrence of carbonate precipitation.

Fig. 5b shows that the slope 1.24 was calculated from the linear regression of $TA_{precipitation}$ against missing C for the first 6 d incubation. The expected ratio should be 1.84 (2:1 – 17/106) due to precipitation and photosynthesis that takes up NO_3^-, which produces 17 mol TA per 106 mol DIC uptake. The underestimation of $TA_{precipitation}$ due to the measurement of TA without removing the effect of algal flocculation on TA_{end} (Danquah et al. 2009, Smith & Davis 2012) could result in the lower calculated ratio of TA reduced to missing C. Some algae, such as coccolithophores, can also acquire CO_2 by releasing CO_2 from calcium carbonate precipitation (Paasche 2001), but this biological calcification is strongly inhibited as POC production is prioritized over particulate inorganic carbon production under C limitation (Bach et al. 2013). Furthermore, diatoms dominated the phytoplankton community in both Delaware Bay and the Pearl River Estuary (Huang et al. 2004, Pan et al. 2011), which is consistent with large amounts of consumed Si during the incubations (Table 1). Coccolithophorids had little

Table 3. Increase in aragonite saturation state (Ω_{arag}) values during incubation in high-salinity (H-Sal), moderate-salinity (M-Sal) and low-salinity (L-Sal) waters in Delaware Bay and the Pearl River Estuary. Initial and end values are from the beginning and end of incubation, respectively; + indicates nutrient additions. Ω_{arag} values were calculated with CO2SYS with measured pH, dissolved inorganic carbon and constants of Millero (2010) (temperature = 25°C)

		H-Sal	H-Sal+	M-Sal	M-Sal+	L-Sal	L-Sal+
Delaware Bay	Initial	2.16	2.94	1.26	1.42	0.02	0.18
	End	5.20	12.05	5.06	10.20	0.97	1.98
Pearl River Estuary	Initial	2.20	6.70	1.32	5.08	0.24	2.53
	End	5.04	9.09	6.45	12.88	5.79	9.92

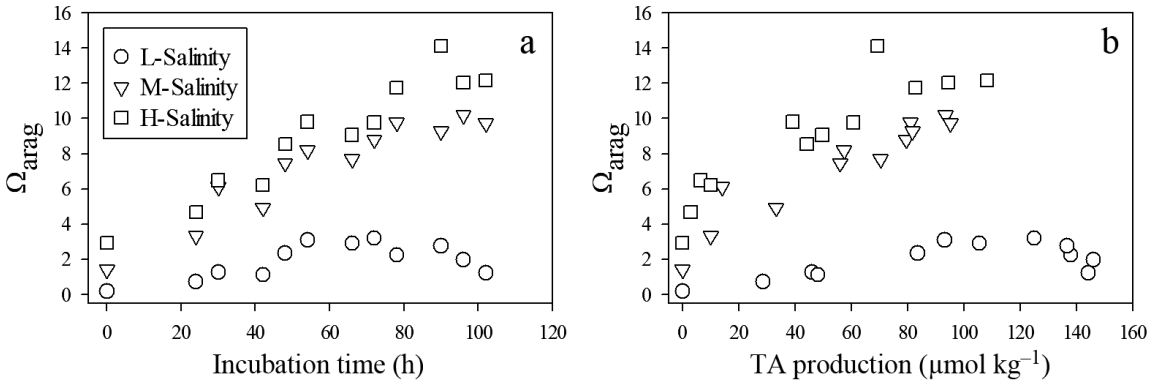

Fig. 6. (a) Changes in aragonite saturation state (Ω_{arag}) values during incubation in 3 water salinities (low, L; moderate, M; high, H) and (b) relationships between Ω_{arag} and total alkalinity (TA) production in Delaware Bay with nutrient additions. Ω_{arag} values were calculated with CO2SYS with measured pH, dissolved inorganic carbon and constants of Millero (2010) (temperature = 25°C); TA production was calculated on nitrogen consumption

contribution to the precipitation, as they were low in abundance, and the mechanism of releasing CO_2 in this study is different from biological calcification.

To test the roles of carbonate precipitation in regulating TA and pH during the phytoplankton blooms, a quantitative model based on CO2SYS was built to simulate the experimental data. We simulated the change in TA and pH with 2 scenarios: with or without carbonate precipitation formation. In the no carbonate precipitation formation case, DIC is only consumed by photosynthesis, and 106 mol of DIC consumption increases TA by 17 mol (Eqs. 1 & 2). In the carbonate precipitation formation case, DIC is consumed by both photosynthesis and carbonate precipitation. In this case, the simulation processes include 2 stages. In stage 1, TA increases and DIC decreases at 17:106 as the photosynthesis consumption ratio. In stage 2, the change in TA and DIC results from both photosynthetic consumption and carbonate precipitation formation. The TA:DIC change ratios are $(-17{:}106) + (2{:}1)_x$, where x is variable, gradually increasing from 0 as the amount of carbonate precipitation formation increases. The changes in the TA:DIC ratio are presented in a conceptual figure (inset in Fig. 7a). As the released CO_2 by carbonate precipitation formation is taken up immediately by photosynthesis, the overall TA:DIC change ratio is less than 2:1.

We ran the model with the change in DIC and TA in the above 2 scenarios, and the measured initial TA and DIC were used as starting values. In stage 1, simulated TA and pH in the carbonate precipitation for-

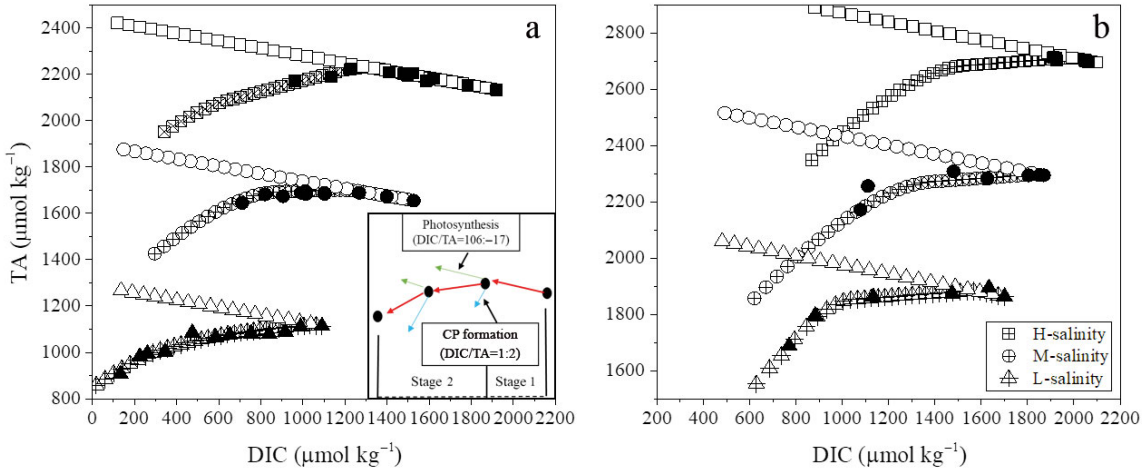

Fig. 7. Comparisons of model-simulated total alkalinity (TA) without (open symbols) and with (cross-filled symbols) carbonate precipitation (CP) formation vs. dissolved inorganic carbon (DIC), and measured TA (solid symbols) in (a) Delaware Bay and (b) the Pearl River Estuary. Simulations were carried out with CO2SYS with constants of Millero (2010) (temperature = 25°C). Inset in the lower-right corner of (a) illustrates the effects of photosynthesis (green arrows) and precipitation (blue arrows) on TA:DIC ratios during phytoplankton blooms. H: high; M: moderate; L: low

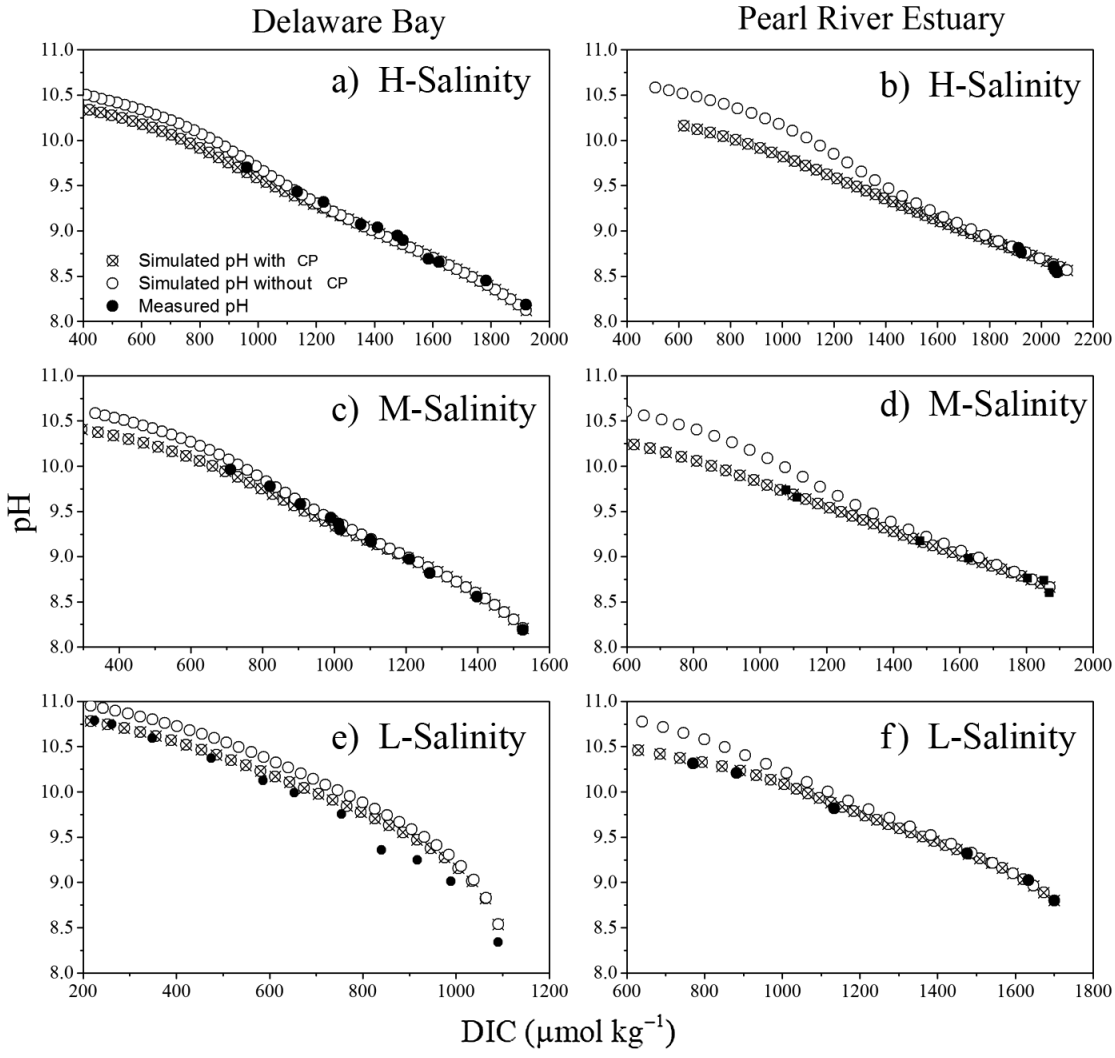

Fig. 8. Comparisons of model-simulated pH without and with carbonate precipitation (CP) formation and measured pH in (a,c,e) Delaware Bay and (b,d,f) the Pearl River Estuary. Open and cross-filled open symbols indicate simulated pH without and with CP formation, respectively; solid symbols indicate the measured pH. Simulations were carried out with CO2SYS with constants of Millero (2010) (temperature = 25°C). DIC: dissolved inorganic carbon; H: high; M: moderate; L: low

mation scenario and in the no carbonate precipitation formation scenario both agreed well with measured TA (Fig. 7) and pH (Fig. 8) in Delaware Bay and the Pearl River Estuary. This means there is no carbonate precipitation formation when DIC is sufficient and pH is low, and the total consumed DIC is utilized by photosynthesis and transferred into POC and DOC. In stage 2, simulated TA and pH in the carbonate precipitation formation scenario agreed well with measured TA and pH (both were lower than those in the no carbonate precipitation formation scenario), and this difference was amplified when more DIC was deposited (x increased) (Figs. 7 & 8), indicating the formation of carbonate precipitation accounts for missing C and the decrease in TA. In addition, the formation of carbonate precipitation decreases pH, reducing the increase in pH promoted by photosynthesis (Fig. 8).

The formation of carbonate precipitation could have released CO_2, and the released CO_2 could have been taken up immediately by phytoplankton for refueling photosynthesis, which could further drive pH higher. Because of the different buffering capacity, the amount of carbonate precipitation formation varied in the 3 water salinities. In the high-salinity waters with high buffering capacity, the changes in TA in the experiments stayed in stage 1 in the Pearl River Estuary and just reached early stage 2 in Delaware Bay, with no or only a small amount of carbonate precipitation formation. As the buffering capacity

is weaker in the moderate- and low-salinity water, when pH rose to a certain level, the changes in TA in the experiments all reached stage 2, resulting in a large amount of carbonate precipitation formation, particularly in low-salinity water. In turn, more carbonate precipitation formation indicates more CO_2 released to fuel the photosynthesis, resulting in higher pH. Therefore, the level of pH regulated by this mechanism depends on the water buffering capacity, enhancing from high buffering capacity seawater to low buffering capacity freshwater in an estuary.

In nature, as reviewed by Zhu & Dittrich (2016), microorganisms can induce carbonate precipitation by altering solution chemistry through a wide range of physiological activities. Effects of eutrophication and ocean acidification on phytoplankton growth and succession might affect future trophic dynamics (Flynn et al. 2015, Zhang et al. 2018). In this study, a large amount of Si was consumed during the incubation (Table 1), indicating that diatoms may dominate the phytoplankton community. As we know, diatoms easily sink into the bottom layer, which can increase biological pump efficiency, causing the formation of hypoxia in the bottom layer. Though grazing activity was ignored in this study, microzooplankton, the major grazers of phytoplankton, can be sensitive to elevated pH (Cripps et al. 2014). Thus, future study on the extent of organic production and its fate during phytoplankton blooms in eutrophic estuaries needs to consider the dynamic interplay between primary and secondary producers grown under variable pH and water buffering capacity and their physiological mechanisms to cope with these dynamics.

5. CONCLUSIONS

In an estuary, water buffering capacity weakens from high- to low-salinity waters, and phytoplankton growth and eutrophication enhance this buffering capacity. High biomass phytoplankton growth stimulated by inorganic eutrophication can result in high pH and formation of carbonate precipitation; the mechanism of CO_2 being released from carbonate precipitation benefits further photosynthesis. This finding has important implications for the biogeochemical processes of carbon in coastal waters. Freshwater from large river outflow is mixed with seawater and spreads over a large area of coastal oceans, for example, in the Pearl River Estuary–South China Sea, Changjiang River Estuary–East China Sea and Mississippi River–Gulf of Mexico. The estuary is a mixture of seawater and freshwater, as we simulated in this study, and thus has a weakened buffering capacity. Phytoplankton blooms often occur in the estuary and result in lower DIC and high pH, which leads to alkalification. The carbonate precipitation formation driven by high pH likely forms mineral precipitates around particles of phytoplankton or detritus, which sink easily into the bottom layer. Thus, alkalification induced by inorganic eutrophication benefits further photosynthesis, and the precipitation can potentially give additional carbon flux during the biological carbon pump process, increasing biological pump efficiency. Furthermore, with greater inorganic eutrophication, coupled with ocean acidification (elevated pCO_2), there may be a potential increase in total phytoplankton bloom size and hypoxia in the estuaries.

Acknowledgements. We acknowledge partial support of a SOA China grant (Key Laboratory for Ecological Environment in Coastal Area 201819). This work is partially supported by a University of Delaware startup fund and an NSF award (OCE-1559279) to W.J.C.'s laboratory, where Y.Z. was a visiting student. This study was part of an NSF-China (91328203) and Guangdong-NSF China joint key project (U1701247). Y.Z. acknowledges financial support from the International Program Fund for PhD candidates, Sun Yat-Sen University (02300-52094201).

LITERATURE CITED

Abril G, Etcheber H, Delille B, Frankignoulle M, Borges AV (2003) Carbonate dissolution in the turbid and eutrophic Loire estuary. Mar Ecol Prog Ser 259:129–138

Bach LT, Mackinder LCM, Schulz KG, Wheeler G, Schroeder DC, Brownlee C, Riebesell U (2013) Dissecting the impact of CO_2 and pH on the mechanisms of photosynthesis and calcification in the coccolithophore *Emiliania huxleyi*. New Phytol 199:121–134

Badger MR, Kaplan A, Berry JA (1980) Internal inorganic carbon pool of *Chlamydomonas reinhardtii*: evidence for a carbon dioxide-concentrating mechanism. Plant Physiol 66:407–413

Björk M, Axelsson L, Beer S (2004) Why is *Ulva intestinalis* the only macroalga inhabiting isolated rockpools along the Swedish Atlantic coast? Mar Ecol Prog Ser 284: 109–116

Borges AV, Gypens N (2010) Carbonate chemistry in the coastal zone responds more strongly to eutrophication than to ocean acidification. Limnol Oceanogr 55:346–353

Cai WJ, Wang ZA, Wang Y (2003) The role of marsh dominated heterotrophic continental margins in transport of CO_2 between the atmosphere, the land–sea interface and the ocean. Geophys Res Lett 30:1849

Cai WJ, Hu X, Huang WJ, Murrell MC and others (2011) Acidification of subsurface coastal waters enhanced by eutrophication. Nat Geosci 4:766–770

Cai WJ, Huang WJ, Luther GW III, Pierrot D and others (2017) Redox reactions and weak buffering capacity lead

to acidification in the Chesapeake Bay. Nat Commun 8:369
Carstensen J, Klais R, Cloern JE (2015) Phytoplankton blooms in estuarine and coastal waters: seasonal patterns and key species. Estuar Coast Shelf Sci 162:98–109
Chen C, Zhu J, Beardsley RC, Franks PJS (2003) Physical–biological sources for dense algal blooms near the Changjiang River. Geophys Res Lett 30:1515
Cloern JE, Foster SQ, Kleckner AE (2014) Phytoplankton primary production in the world's estuarine–coastal ecosystems. Biogeosciences 11:2477–2501
Cripps G, Lindeque P, Flynn KJ (2014) Have we been underestimating the effects of ocean acidification in zooplankton? Glob Change Biol 20:3377–3385
Dai M, Zhai W, Cai WJ, Callahan J and others (2008) Effects of an estuarine plume-associated bloom on the carbonate system in the lower reaches of the Pearl River Estuary and the coastal zone of the northern South China Sea. Cont Shelf Res 28:1416–1423
Danquah MK, Gladman B, Moheimani NR, Forde GM (2009) Microalgal growth characteristics and subsequent influence on dewatering efficiency. Chem Eng J 151:73–78
Doney SC, Mahowald N, Lima I, Feely RA, Mackenzie FT, Lamarque JF, Rasch PJ (2007) Impact of anthropogenic atmospheric nitrogen and sulfur deposition on ocean acidification and the inorganic carbon system. Proc Natl Acad Sci USA 104:14580–14585
Duarte CM, Hendriks IE, Moore TS, Olsen YS and others (2013) Is ocean acidification an open-ocean syndrome? Understanding anthropogenic impacts on seawater pH. Estuaries Coasts 36:221–236
Egleston ES, Sabine CL, Morel FMM (2010) Revelle revisited: buffer factors that quantify the response of ocean chemistry to changes in DIC and alkalinity. Global Biogeochem Cycles 24:GB1002
Feely RA, Alin SR, Newton J, Sabine CL and others (2010) The combined effects of ocean acidification, mixing, and respiration on pH and carbonate saturation in an urbanized estuary. Estuar Coast Shelf Sci 88:442–449
Flynn KJ, Blackford JC, Baird ME, Raven JA and others (2012) Changes in pH at the exterior surface of plankton with ocean acidification. Nat Clim Chang 2:510–513
Flynn KJ, Clark DR, Mitra A, Fabian H and others (2015) Ocean acidification with (de)eutrophication will alter future phytoplankton growth and succession. Proc Biol Sci 282:20142604
Frankignoulle M (1994) A complete set of buffer factors for acid/base CO_2 system in seawater. J Mar Syst 5: 111–118
Frankignoulle M, Canon C, Gattuso JP (1994) Marine calcification as a source of carbon dioxide: positive feedback of increasing atmospheric CO_2. Limnol Oceanogr 39: 458–462
Gao Y, Cornwell JC, Stoecker DK, Owens MS (2014) Influence of cyanobacteria blooms on sediment biogeochemistry and nutrient fluxes. Limnol Oceanogr 59:959–971
Giordano M, Beardall J, Raven JA (2005) CO_2 concentrating mechanisms in algae: mechanisms, environmental modulation, and evolution. Annu Rev Plant Biol 56:99–131
Guo X, Cai WJ, Zhai W, Dai M, Wang Y, Chen B (2008) Seasonal variations in the inorganic carbon system in the Pearl River (Zhujiang) estuary. Cont Shelf Res 28: 1424–1434
Guo X, Dai M, Zhai W, Cai WJ, Chen B (2009) CO_2 flux and seasonal variability in a large subtropical estuarine system, the Pearl River Estuary, China. J Geophys Res 114: G03013
Hansen PJ (2002) Effect of high pH on the growth and survival of marine phytoplankton: implications for species succession. Aquat Microb Ecol 28:279–288
Hansen PJ, Lundholm N, Rost B (2007) Growth limitation in marine red-tide dinoflagellates: effects of pH versus inorganic carbon availability. Mar Ecol Prog Ser 334: 63–71
Hinga KR (2002) Effects of pH on coastal marine phytoplankton. Mar Ecol Prog Ser 238:281–300
Howarth RW (1988) Nutrient limitation of net primary production in marine ecosystems. Annu Rev Ecol Evol Syst 19:89–110
Huang L, Jian W, Song X, Huang X and others (2004) Species diversity and distribution for phytoplankton of the Pearl River estuary during rainy and dry seasons. Mar Pollut Bull 49:588–596
Huang WJ, Wang Y, Cai WJ (2012) Assessment of sample storage techniques for total alkalinity and dissolved inorganic carbon in seawater. Limnol Oceanogr Methods 10:711–717
Joesoef A, Huang WJ, Gao Y, Cai WJ (2015) Air–water fluxes and sources of carbon dioxide in the Delaware Estuary: spatial and seasonal variability. Biogeosciences 12:6085–6101
Joesoef A, Kirchman DL, Sommerfield CK, Cai WJ (2017) Seasonal variability of the inorganic carbon system in a large coastal plain estuary. Biogeosciences 14:4949–4963
Kauffman GJ, Homsey AR, Belden AC, Sanchez JR (2011) Water quality trends in the Delaware River Basin (USA) from 1980 to 2005. Environ Monit Assess 177:193–225
Knap A, Michaels A, Close A, Ducklow H, Dickson A (eds) (1996) Protocols for the joint global ocean flux study (JGOFS) core measurements. JGOFS Report No. 19, Reprint of IOC Manuals and Guides No. 29, UNESCO 1994
Lu Z, Gan J (2015) Controls of seasonal variability of phytoplankton blooms in the Pearl River Estuary. Deep Sea Res II 117:86–96
Middelboe AL, Hansen PJ (2007) Direct effects of pH and inorganic carbon on macroalgal photosynthesis and growth. Mar Biol Res 3:134–144
Millero FJ (2010) Carbonate constants for estuarine waters. Mar Freshw Res 61:139–142
Paasche E (2001) A review of the coccolithophorid *Emiliania huxleyi* (Prymnesiophyceae), with particular reference to growth, coccolith formation, and calcification–photosynthesis interactions. Phycologia 40:503–529
Pan X, Mannino A, Marshall HG, Filippino KC, Mulholland MR (2011) Remote sensing of phytoplankton community composition along the northeast coast of the United States. Remote Sens Environ 115:3731–3747
Pierrot D, Lewis E, Wallace D (2006) MS Excel program developed for CO_2 system calculations. ORNL/CDIAC-105a, Carbon Dioxide Inf Anal Cent, Oak Ridge Natl Lab, US Dep Energy, Oak Ridge, TN
Raven JA (1970) Exogenous inorganic carbon sources in plant photosynthesis. Biol Rev Camb Philos Soc 45: 167–220
Reinfelder JR (2011) Carbon concentrating mechanisms in eukaryotic marine phytoplankton. Annu Rev Mar Sci 3: 291–315
Sharp JH, Yoshiyama K, Parker AE, Schwartz MC and others (2009) A biogeochemical view of estuarine eutrophication: seasonal and spatial trends and correlations

in the Delaware Estuary. Estuaries Coasts 32:1023–1043
Smith BT, Davis RH (2012) Sedimentation of algae flocculated using naturally-available, magnesium-based flocculants. Algal Res 1:32–39
Soetaert K, Hofmann AF, Middelburg JJ, Meysman FJR, Greenwood J (2007) The effect of biogeochemical processes on pH. Mar Chem 105:30–51
Vandamme D, Foubert I, Fraeye I, Meesschaert B, Muylaert K (2012) Flocculation of *Chlorella vulgaris* induced by high pH: role of magnesium and calcium and practical implications. Bioresour Technol 105:114–119
Verschoor AM, Van Dijk MA, Huisman J, Van Donk E (2013) Elevated CO_2 concentrations affect the elemental stoichiometry and species composition of an experimental phytoplankton community. Freshw Biol 58:597–611
Verspagen JMH, Van De Waal DB, Finke JF, Visser PM, Van Donk E, Huisman J (2014) Rising CO_2 levels will intensify phytoplankton blooms in eutrophic and hypertrophic lakes. PLOS ONE 9:e104325
Wang ZA, Wanninkhof R, Cai WJ, Byrne RH, Hu X, Peng TH, Huang WJ (2013) The marine inorganic carbon system along the Gulf of Mexico and Atlantic coasts of the United States: insights from a transregional coastal carbon study. Limnol Oceanogr 58:325–342
Wolf-Gladrow DA, Zeebe RE, Klaas C, Körtzinger A, Dickson AG (2007) Total alkalinity: the explicit conservative expression and its application to biogeochemical processes. Mar Chem 106:287–300
Yin K (2003) Influence of monsoons and oceanographic processes on red tides in Hong Kong waters. Mar Ecol Prog Ser 262:27–41
Yin K, Harrison PJ (2008) Nitrogen over enrichment in subtropical Pearl River estuarine coastal waters: possible causes and consequences. Cont Shelf Res 28:1435–1442
Yin K, Song X, Sun J, Wu MCS (2004) Potential P limitation leads to excess N in the Pearl River estuarine coastal plume. Cont Shelf Res 24:1895–1907
Zhang Y, Song X, Harrison PJ, Liu S and others (2018) Regeneration and utilization of nutrients during collapse of a *Mesodinium rubrum* red tide and its influence on phytoplankton species composition. Sci China Earth Sci 61:1384
Zhu T, Dittrich M (2016) Carbonate precipitation through microbial activities in natural environment, and their potential in biotechnology: a review. Front Bioeng Biotechnol 4:4

Editorial responsibility: Steven Lohrenz, New Bedford, Massachusetts, USA

Submitted: April 23, 2018; Accepted: November 30, 2018
Proofs received from author(s): January 13, 2019